Chemical Engineering Journal 534 (2026) 174476

Contents lists available at ScienceDirect

Chemical Engineering Journal

journal homepage: www.elsevier.com/locate/cej

Ion-specific control of chlorine hydrolysis in concentrated NaCl and $NaClO_4$ solutions

Lewis A.D. Waller [a,b], Andrea E. Russell [a], Peter P. Wells [a], Richard G. Wills [b], Robert Raja [a], Lindsay-Marie Armstrong [b,*]

[a] School of Chemistry and Chemical Engineering, University of Southampton, Southampton, United Kingdom
[b] Department of Mechanical Engineering, University of Southampton, Southampton, United Kingdom

ARTICLE INFO

Keywords:
Chlorine hydrolysis
Chlor-alkali process
Pitzer model
Activity coefficients
Ionic strength

ABSTRACT

Thermodynamic descriptions of the chlor-alkali process are sensitive to the treatment of chlorine hydrolysis under concentrated electrolyte conditions. Reported equilibrium constants for this reaction exhibit meaningful variation when extrapolated from dilute solutions, complicating comparison between studies and introducing uncertainty into process-relevant speciation calculations. In this work, UV–Vis spectroscopy is combined with a Pitzer-based thermodynamic framework to examine chlorine hydrolysis in aqueous sodium perchlorate and sodium chloride electrolytes across industrially relevant ionic strengths ($0.028 \leq I_m \leq 2.1$ mol kg^{-1}) at 298.15 K. A thermodynamically consistent reference value for the chlorine hydrolysis is adopted and used to quantify electrolyte-dependent non-ideal effects through explicit treatment of ionic activity coefficients and water activity. The analysis separates the competing contributions of electrostatic stabilisation and solvent activity suppression, yielding a non-monotonic dependence of the equilibrium position on ionic strength. Comparison of chloride and perchlorate media at matched ionic strengths demonstrates that equilibrium shifts cannot be described by ionic strength alone but depend on electrolyte identity through ion-solvent and ion-ion interactions. The experimental measurements are consistent with the framework in both electrolytes, providing a structured basis for interpreting chlorine hydrolysis in concentrated aqueous systems and for reconciling historical equilibrium data under non-ideal conditions.

Nomenclature

Symbol	Description	Units
A_λ	Absorbance at wavelength λ	–
a_w	Activity of water	–
m_j	Molal concentration of species j	mol kg^{-1}
I_m	Ionic strength	mol kg^{-1}
$[X]$	Molal concentration of species X	mol kg^{-1}
$[X]_0$	Initial molal concentration of species X	mol kg^{-1}
$[X]_\infty$	Equilibrium molal concentration of species X	mol kg^{-1}
K^c	Concentration-based equilibrium constant	Reaction dependent
K^Θ	Thermodynamic Equilibrium constant	–
l	Optical path length	cm
Greek Symbols		
Γ	Activity coefficient quotient	–
γ	Molal activity coefficient of a species	–
$\varepsilon_{j,\lambda}$	Molar extinction coefficient of species j at wavelength λ	L mol^{-1} cm^{-1}

1. Introduction

A major commercial source of chlorine gas is the chlor-alkali process [1,2], Eqs. 1–3, an electrochemical process requiring 2200–2600 kWh of electricity per tonne of chlorine produced [2,3]. Globally, the chlor-alkali process consumes an estimated 220–265 TWh annually [4,5]; nearly 1.0% of global electricity consumption [3,6]. Reflecting its industrial significance, global chlorine demand was estimated at 106 Mt. in 2024, with projections reaching 128 Mt. by 2030 [7]; increasing energy demand by 63–70 TWh, underscoring the need for scalable process optimisation to reduce environmental impacts [8].

$$\text{Anode}: \quad 2Cl^- \rightarrow Cl_{2\,(g)} + 2e^- \tag{1}$$

* Corresponding author at: School of Mechanical Engineering, University of Southampton, Southampton, United Kingdom.
E-mail address: l.armstrong@soton.ac.uk (L.-M. Armstrong).

https://doi.org/10.1016/j.cej.2026.174476
Received 1 December 2025; Received in revised form 13 February 2026; Accepted 21 February 2026
Available online 24 February 2026

$$\text{Cathode}: \quad 2H_2O + 2e^- \rightarrow 2OH^- + H_{2\,(g)} \tag{2}$$

$$\text{Overall}: \quad 2NaCl + 2H_2O \rightarrow Cl_{2\,(g)} + H_{2\,(g)} + NaOH \tag{3}$$

Once generated by the chlor-alkali process, Eqs. 1–3, chlorine undergoes hydrolysis (Eq. 4) [1,9]. Unless stated otherwise, all species are aqueous; Cl_2 refers specifically to dissolved molecular chlorine.

$$Cl_2 + H_2O \leftrightharpoons H^+ + Cl^- + HOCl \tag{4}$$

This equilibrium governs chlorine speciation, impacting reactor efficiency within chlor-alkali systems and determining the relative concentrations of active chlorine species (Cl_2, HOCl). These species dictate reaction pathways and product selectivity in chemical synthesis [10–14], efficacy in water treatment and disinfection [10,14–16], and the overall performance of chlorine-based disinfectant formulations [16]. Consequently, precise control and accurate estimation of this reaction equilibrium are essential for the optimisation and sustainability of chlorine-related processes.

Despite extensive experimental studies of chlorine hydrolysis [17–21], reported values of the thermodynamic equilibrium constants for chlorine hydrolysis (K^{Θ}) differ meaningfully (Table 1). In many of these studies, ionic strength was controlled using perchlorate-based electrolytes (e.g., $NaClO_4$ or $HClO_4$), selected for their inertness, whereas industrial and applied systems predominantly involve chloride-rich brines or mixed electrolytes. [22,23] The deviations become magnified under industrially relevant ionic strengths ($I_m > 0.5$ mol kg^{-1}), primarily because historical studies often rely on dilute-solution approximations or implicit treatments of non-ideality that are not transferable between different background electrolytes. [14,24–30] Such approaches tend to obscure the separate contributions of electrostatic interactions and solvent activity; consequently, agreement at low ionic strength does not ensure accuracy in concentrated mixed brines. As we later demonstrate, these variations lead to significant deviations in predicted chlorine speciation for process applications. To address this, the present work applies a single, internally consistent thermodynamic framework that explicitly resolves electrolyte-specific non-ideal effects while maintaining a fixed reference equilibrium constant.

To develop a consistent approach, we combine UV–Vis spectroscopy with a Pitzer ion-interaction framework [31–34] (Eqs. S1-S17) that accounts for binary and ternary interactions across a broad range of industrially relevant ionic strengths ($I_m \leq 6.0$ mol kg^{-1}). The framework's resulting description of chlorine hydrolysis equilibrium constants are compared with new measurements in $NaClO_4$ ($0.028 \leq I_m \leq 2.1$ mol kg^{-1}) and NaCl ($0.076 \leq I_m \leq 0.83$ mol kg^{-1}), directly quantifying Cl_2, HOCl and Cl_3^- concentrations. The experimental and computational methods have been explained in detail in the Supporting Information.

Pitzer-type models are semi-empirical with key limitations. Their formulation rests on the assumption that the total excess Gibbs energy (ΔG_m^{ex}), which defines non-ideal behaviour, arises from binary and, to a much lesser extent ternary ion-ion interactions. This simplification neglects the self-interaction of ions (e.g., $Na^+ - Na^+$, $Mg^{2+} - Mg^{2+}$) as well as quaternary and further higher-order interactions. Such effects can become significant in complex systems, for example, those involving hydrophobic ionic species or clathrate-forming species [35]. While this assumption is appropriate for the present system, more complex electrolytes may require models that incorporate higher-order terms.

As a semi-empirical approach, Pitzer-type models rely on parameters obtained from regression of experimental data, and their accuracy is therefore constrained by the availability and quality of those datasets. While industrial chlor-alkali electrolysis typically operates at elevated temperatures (approx. $80 - 90$°C) [22,36–38], the high-precision experimental data required for robust parameterisation are predominantly at 298.15 K. Extrapolation to industrial temperatures using the currently sparse high-temperature data introduces significant uncertainty. [39–41] Accordingly, the present study is restricted to 298.15 K and is intended to establish a thermodynamically consistent reference state against which non-ideal effects can be resolved. Such a reference state is necessary for the interpretation of concentrated electrolyte behaviour in downstream processing, environmental dispersion scenarios, and emerging low-temperature chlor-alkali research. [38] Extension of the framework to elevated operating temperatures would require future extension of the framework through targeted high-temperature measurements to preserve the same level of thermodynamic consistency.

The framework is therefore not presented as an ab initio prediction, but as a thermodynamically consistent tool for interpreting experimental data within a well-defined system. Within this context, the Pitzer model provides a practical means of evaluating the necessary activity coefficients and solvent activity using existing interaction parameters. Moreover, given the extensive literature database of Pitzer interaction parameters, this framework enables computational screening of diverse electrolyte backgrounds to identify optimal reaction environments prior to experimental validation. This allows the specific influence of the background electrolyte composition (e.g., NaCl vs $NaClO_4$) to be modelled, enabling electrolyte-specific equilibrium shifts to be resolved without re-fitting reaction parameters. However, for systems where such parameters are missing (e.g., iodine hydrolysis), they would first need to be derived from new experimental data. Extensive discussion of the broader limitations of Pitzer-type models is available within the literature [39–41].

Table 1
Selected literature values of the thermodynamic equilibrium constant for chlorine hydrolysis.

Temperature (°C)	$K^{\Theta} \times 10^4$	I_m (mol kg^{-1})	Method	Ref.
25	3.944	< 0.03	Conductance	[17]
25	3.35	1.0	UV–Vis	[18]
25	3.88	0.1	Temperature jump	[19]
25	4.02 – 4.16	< 2.85	UV–Vis	[20]
25	5.05	0.5	Stopped flow	[21]

Note: In all historical studies, $NaClO_4$ was used to adjust for ionic strength.

2. Experimental and modelling overview

Chlorine Hydrolysis equilibria were quantified under purely chemical equilibrium conditions using UV–Vis absorption spectroscopy at 298.15 K in pre-prepared aqueous sodium perchlorate (reagent grade, >98.0%) and sodium chloride (reagent grade, >99.0%) electrolytes over a range of ionic strengths ($0.028 \leq I_m \leq 2.133$). Unless otherwise stated, all materials were sourced from Sigma Aldrich. Hydrochloric acid (0.1 N) and sodium hypochlorite (6–14% active chlorine) were added in controlled amounts to the pre-prepared electrolyte solutions to establish the desired initial chlorine speciation prior to equilibration.

Equilibrium concentrations of dissolved chlorine, hypochlorous acid, and trichloride were obtained from Beer-Lambert analysis using wavelength-resolved molar extinction coefficients and full mass-balance constraints. For each experiment, the equilibrium concentration of dissolved molecular chlorine was treated as the sole adjustable parameter and determined by weighted least-squares fitting of measured spectra. Because Cl_3^- contributes strongly to absorbance in the fitted spectral window, the UV–Vis inversion requires one additional closure condition; here this was provided by fixing $K_{Cl_3^-}$ to the literature value 0.18 [42] across all experiments.

Non-ideal solution behaviour was accounted for using a Pitzer ion-interaction framework; developed in-house using Python, to calculate

ionic activity coefficients and water activity as functions of electrolyte composition and ionic strength.

Activity coefficients for charged species and solvent activity were evaluated explicitly, while neutral species were approximated with unit activity coefficients, consistent with their low concentrations and the absence of reported interaction parameters. Concentration-based equilibrium quotients were converted to thermodynamic equilibrium constants using the calculated activity ratios. Single-ion activity coefficients are used here as model resolved thermodynamic quantities within the adopted convention, not as directly measurable observables. Accordingly, model verification is based on measurable composite quantities: UV–Vis-derived equilibrium concentrations, concentration-based equilibrium quotients, and agreement with literature mean HCl activity/activity-ratio trends.

Uncertainties in equilibrium constants were determined from regression statistics and propagated through the activity corrections; all reported uncertainties correspond to 95% confidence limits unless otherwise stated. The full experimental procedure, thermodynamic equations, parameter sources, and data tables are provided in the Supporting Information.

3. Results and discussion

3.1. Evaluation of the Pitzer framework

Equilibrium constants reported in the literature are commonly defined as thermodynamic equilibrium constants (K^{Θ}) on an activity basis (a_i), which reference ideal conditions, facilitating comparisons across different experimental setups. These K^{Θ} values are inferred by extrapolating measurements made at finite ionic strength to the standard state and therefore reflect equilibrium under ideal conditions. The relationship between the thermodynamic (K^{Θ}) and concentration-based equilibrium constants (K^{c}) at non-zero ionic strengths is defined by Eq. 5:

$$K^{\Theta} = \frac{\prod a_{\text{products}}}{\prod a_{\text{reactants}}} \tag{5}$$

$$a_i = \gamma_i \times m_i \tag{6}$$

$$K^{\Theta} = K^{c} \times \Gamma = \frac{\prod m_{\text{products}}}{\prod m_{\text{reactants}}} \times \frac{\prod \gamma_{\text{products}}}{\prod \gamma_{\text{reactants}}} \tag{7}$$

Here, the concentrations, m_i, in K^{c} are expressed as dimensionless ratios normalised by the molality standard state (m_i/m^0, with $m^0 = 1\ \text{mol kg}^{-1}$), such that K^{c} is dimensionless by convention. The factor Γ accounts for non-ideal solution behaviour via ion activity coefficients (γ). For the chlorine hydrolysis reaction, the full activity quotient, Γ, includes contributions from all reacting species and the solvent.

Activity coefficients for the neutral species, Cl_2 and HOCl are approximated as unity, as Pitzer interaction parameters for these components are unavailable in the literature. In concentrated electrolyte solutions, non-ideal behaviour is dominated by electrostatic ion-ion interactions and by deviations in solvent activity, while contributions from neutral species to the excess Gibbs energy are comparatively small. [32] Under the acidic conditions investigated, hypochlorous acid remains largely undissociated, and the equilibrium position is governed primarily by the activities of H^+ and Cl^- together with water activity. Accordingly, explicit treatment of charged species and solvent activity captures the dominant thermodynamic controls on the chlorine hydrolysis equilibrium within the concentration range examined. Further discussion on this assumption can be found in the Supplementary Information.

$$K^{\Theta} = \frac{[\text{HOCl}][\text{H}^+][\text{Cl}^-]}{[\text{Cl}_2][\text{H}_2\text{O}]} \times \frac{\gamma_{\text{HOCl}} \times \gamma_{\text{H}^+} \times \gamma_{\text{Cl}^-}}{\gamma_{\text{Cl}_2} \times \gamma_{\text{H}_2\text{O}}} \tag{8}$$

This approximation is consistent with the treatment adopted in prior studies of chlorine hydrolysis [17,21,43]. While salting-out effects in concentrated electrolytes may lead to in $\gamma > 1$ [44], such effects influence both Cl_2 and HOCl and therefore exert opposing contributions to the equilibrium quotient; these effects partially offset and do not alter the dominant thermodynamic trends resolved here.

With this simplification, the thermodynamic equilibrium constant (Eq. 8) may be expressed as:

$$K^{\Theta} = \frac{[\text{HOCl}][\text{H}^+][\text{Cl}^-]}{[\text{Cl}_2]} \times \frac{\gamma_{\text{H}^+} \times \gamma_{\text{Cl}^-}}{a_{\text{H}_2\text{O}}} \tag{9}$$

The activity ratio (K^{c}/K^{Θ}), which isolates the contribution of non-ideality, thus becomes:

$$\frac{K^{c}}{K^{\Theta}} = \Gamma^{-1} = \frac{a_{\text{H}_2\text{O}}}{\gamma_{\text{H}^+} \times \gamma_{\text{Cl}^-}} \tag{10}$$

Γ^{-1} quantifies the cumulative effect of ionic strength on the equilibrium through its influence on ion activity coefficients (γ_i) and solvent activity (a_{H_2O}). In the present work, the Pitzer framework is applied to evaluate this ratio by explicitly separating electrostatic stabilisation, solvent activity suppression, and specific-ion effects without re-parameterising the reaction constant.

Before applying this framework to the chlorine hydrolysis data, internal consistency was assessed. As previously discussed, the Pitzer model is semi-empirical, and its parameters are derived from regression of experimental data. Therefore, comparison with literature data (Fig. 1) does not constitute independent validation [45]; agreement is expected since the parameters are derived from similar datasets. Rather, this step is a necessary assessment to demonstrate the self-consistency of the chosen parameter set. The complete theoretical expressions and parameters sources are given in the Supporting Information (Eqs. S1-S17 and Table S1-S2).

The model's ability to describe bulk-solution behaviour was first examined through comparison with relevant literature data (Fig. 1). Fig. 1A shows the assessment of solvent activity (a_w), comparing calculated water activity with experimental measurements from Silverman [20] in a reactive chlorine hydrolysis system at 298.15 K, with ionic strength adjusted using $NaClO_4$. Given the low molalities of H^+ and Cl^- compared with $NaClO_4$ in these systems, the reduction in water activity is attributed primarily to hydration of Na^+ and ClO_4^- ions. The model's description aligns with the experimental data within expected uncertainty.

A complementary assessment of solute activity was performed using historical measurements from non-reactive proxy systems ($NaClO_4 - HCl - H_2O$) at 298.15 K. These systems containing trace HCl in concentrated $NaClO_4$, allow for the evaluation of specific ion interactions without the complication of ongoing reactions. The model reproduced literature trends for HCl activity across the examined range ($I_m \leq 3.5\ \text{mol kg}^{-1}$), as shown in Fig. 1B, demonstrating internal consistency within the framework.

Finally, the individual model-derived components ($\gamma_{H^+}, \gamma_{Cl^-}$ and a_w) for the non-reactive proxy system were incorporated into Eq. 10 to calculate the activity ratio (Γ^{-1}). Fig. 1C compares calculated values with experimental data from the $NaClO_4$ systems taken from various literature sources [46–48]. The general agreement across the ionic strength range examined ($I_m \leq 3.5\ \text{mol kg}^{-1}$) suggests that the framework reproduces the observed thermodynamic trends for mixed electrolytes within the anticipated constraints and capabilities of the model. The use of proxy system data to characterise activity coefficients is justified by the following rationale: $NaClO_4$ is commonly used to adjust ionic strength in chlorine hydrolysis studies [20,21] because it does not participate in the reaction. When $NaClO_4$ concentration greatly exceeds that of the reactive species (Cl_2, HOCl, HCl), the specific ion interactions governing HCl activity coefficients in the proxy system ($NaClO_4 - HCl - H_2O$) closely approximate those in the reactive

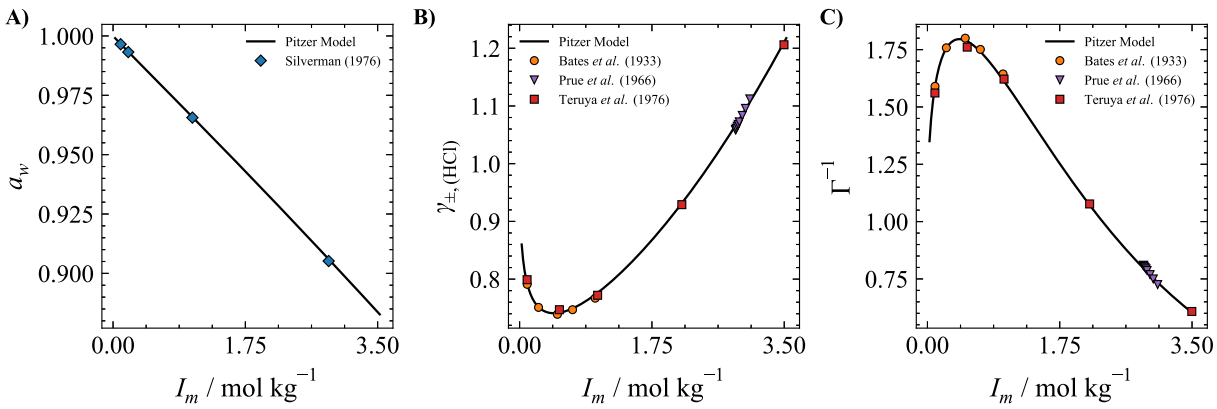

Fig. 1. Calculated thermodynamic properties of electrolyte systems using the Pitzer framework. Ionic strength was varied by $NaClO_4$ concentration at 298.15 K. (A) Water activity compared with experimental data from Silverman (1976) [20] in reactive chlorine hydrolysis systems. (B) Calculated trace HCl activity coefficients in HCl-$NaClO_4$ proxy systems (1:100 M ratio). (C) Corresponding activity ratios derived from the same framework. Experimental data for (B) and (C) are from literature sources of comparable systems [46–48].

system. The model's reproduction of measured activity ratios under these conditions indicates that it can estimate equilibrium shifts arising from ionic strength effects.

This approach can be extended to other background electrolytes. For example, if chlorine hydrolysis were studied in NaCl medium, the associated activity effects could be estimated from $HCl - NaCl - H_2O$ data, provided the NaCl concentration significantly exceeds that of the reactive species. Experimental confirmation of this transferability would enable systematic screening of electrolyte compositions to identify ionic environments that enhance or stabilise chlorine hydrolysis.

3.2. *Re-examination of historical data and underlying thermodynamic effects*

A re-examination of key historical data for chlorine hydrolysis was conducted. This sought to identify the origins of reported differences in equilibrium constants and to quantify the impact of these uncertainties on process modelling. Investigation of the literature revealed differences in the derived equilibrium constants reported by Eigen et al. [19] and Wang et al. [21].

Eigen et al. reported a concentration-based constant of $K^c = 6.10 \times 10^{-4}$ ($I_m = 0.1$ mol kg^{-1}), having derived this value from the kinetic data from Connick et al. [17], by establishing a thermodynamic constant (K^{Θ}), adjusting it to 20°C ($K^{\Theta} = 3.88 \times 10^{-4}$), and correcting for ionic strength using the Davies Equation (Eq. [49]). However, re-evaluation of Connick et al.'s dataset (Fig. 2) suggests that a graphical extrapolation step in Eigen's treatment likely introduced a numerical offset. At 20°C, a lower thermodynamic equilibrium constant ($K^{\Theta} = 3.31 \times 10^{-4}$) is expected. When adjusted for ionic strength ($I_m = 0.1$ mol kg^{-1}) using the Davies Equation (Eq. [49]), the resulting K^c is 5.53×10^{-4}. This recalculation brings the result into closer agreement with subsequent measurements. Consequently, this corrected value is adopted for the remainder of this work.

Similarly, the study of Wang et al. [21], presents a thermodynamic equilibrium constant of $K^{\Theta} = 5.05 \times 10^{-4}$ at 298.15 K, a value attributed to Bard et al. [50]. As illustrated in Fig. 2, this reported constant is approximately 29% higher than the value derived from Connick et al. [17] at 298.15 K, the variation most likely reflects differences in data selection or the specific conventions applied in the calculation rather than a fundamental discrepancy. Wang et al. [21] applied ionic-strength corrections assuming non-ideal effects acted though γ_{H^+} and γ_{Cl^-}, while treating water activity implicitly. While this represented a valid approximation at the time, recent approaches, including the Pitzer framework used here, explicitly incorporate water-activity and mixed-electrolyte effects, offering an alternative route to assess these results.

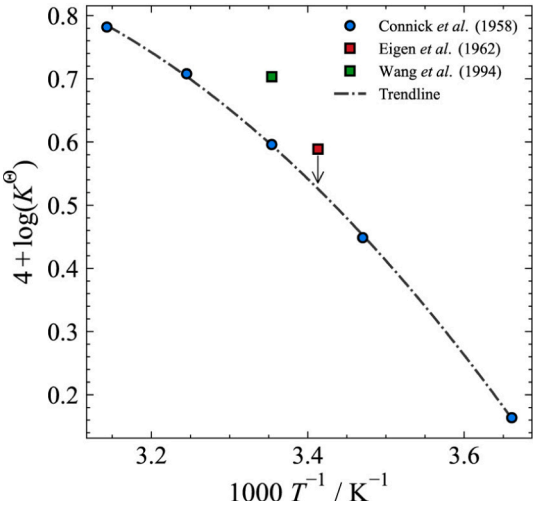

Fig. 2. Thermodynamic equilibrium constants for chlorine hydrolysis, showing data from Connick et al. [17], Eigen et al. [19] and Wang et al. [21]. The figure is adapted from Connick et al. [17].

The datasets of Eigen et al. [19] and Wang et al. [21] remain widely cited in studies of chlorine hydrolysis and related aqueous systems [27,29,30,51]. Their enduring use underscores the importance of periodically revisiting foundational data with updated thermodynamic formalisms.

Thermodynamic equilibrium constants reported in the literature are defined at the standard state and therefore correspond to zero ionic strength. However, these values are inferred from experimental measurements conducted at finite ionic strength, and their accuracy depends on the treatment of non-ideal solution behaviour employed in each study. Zimmerman et al. inferred K^{Θ} from measurements in HCl-$HClO_4$ mixtures at a fixed ionic strength of 1 mol kg^{-1} [18], Wang et al. from measurements in $NaClO_4$ at an ionic strength of 0.5 mol kg^{-1} [21], while Connick et al. did not employ an inert background electrolyte; with ionic strength arising solely from the generated H^+ and Cl^- ions and remaining typically below 0.03 mol kg^{-1}. [17] Differences in the reported thermodynamic equilibrium constants therefore reflect not only experimental uncertainty, but also the assumptions and corrections used to extrapolate from finite ionic strength to the standard state.

To illustrate the potential influence of these historical variations, a sensitivity analysis was performed under idealised conditions ($[Cl^-] = 0.01$ M unity activity coefficients), with pH defined on an ac-

tivity basis as pH $= -\log_{10}(a_{H^+})$. In this expression, a_{H^+} is represented, within the selected thermodynamic convention, as $m_{H^+}\gamma_{H^+}$. Absolute single-ion activities are not directly measurable; accordingly, pH is used here to enable comparison between model scenarios. This isolates uncertainty arising solely from the choice of K^{Θ} (Fig. 3), as non-ideal effects were omitted. The analysis suggests that the spread in literature values leads to meaningful deviation in predicted speciation. Unlike absolute deviation, which peaks in the transition region, the relative percentage error remains significant across the entire pH range. Under the specific conditions examined here, the difference in literature constants results in a maximum deviation up to 27% relative to the baseline, which propagates directly into errors in predicted active chlorine availability and pH-dependent reaction pathways in reactor-scale models. The re-evaluation presented here therefore seeks to reduce this specific source of variance by establishing a thermodynamically consistent reference constant.

3.3. Thermodynamic drivers of non-ideality

To examine the physical origins of the non-ideal effects influencing the chlorine hydrolysis equilibrium, the Pitzer framework was used to decompose the activity ratio (Γ^{-1}) into its thermodynamic components (Fig. 4A). By comparing the definition including water activity ($\Gamma^{-1} = a_w/\gamma_{H^+}\gamma_{Cl}$) against the ionic-only contribution ($\Gamma^{-1^*} = 1/\gamma_{H^+}\gamma_{Cl}$), it is evident that while solvent activity influences the magnitude, the ionic strength dependence is primarily governed by the mean ionic activity product. An initial rise in Γ^{-1} is anticipated due to the electrostatic stabilisation of the H^+ and Cl^- ions arising from the formation of counter-ion atmospheres in the supporting $NaClO_4$ electrolyte. Quantitative decomposition of the model parameters (Fig. 4C) identifies that this regime dominates below the calculated thermodynamic turning point of $I_m = 0.45$ mol kg^{-1}. In this region ($I_m < 0.45$ mol kg^{-1}), the expansion of counter-ion atmospheres, which are governed by the Debye-Hückel term (f^{γ}), reduces the mean ionic activity coefficients ($\gamma_{\pm}$); for instance, at $I_m = 0.1$ mol kg^{-1}, the gradient of the short-range forces is approximately 47% of the electrostatic gradient.

At ionic strengths exceeding 0.45 mol kg^{-1}, this effect is overcome by short-range repulsive forces and ion-solvent interactions. Differentiation of the mean ionic activity coefficient ($d\ln\gamma_{\pm}/dI_m$) shows that at this turning point, the stabilising electrostatic gradient is counterbalanced by the repulsive gradient ($d\ln\gamma^{SR}/dI_m \approx -d\ln\gamma^{LR}/dI_m$), where SR and LR denote short-range and long-range electrostatic virial contributions, respectively. Beyond this point, the contribution of the Pitzer binary interaction parameters, most notably the hard-core repulsion term $\beta^{(0)}$, increases linearly with molality, driving the decrease in Γ^{-1}. The dominance of these repulsive forces becomes pronounced in the concentrated regime; by $I_m = 3.0$ mol kg^{-1}, the short-range repulsive gradient is 3.3 times larger than the long-range electrostatic effect.

This modulation is further influenced by changes in water activity (a_w), which reflect the extent of solute-solvent interactions. As $NaClO_4$ concentration increases, progressively more water molecules are incorporated into the hydration shells of Na^+ and ClO_4^- [52,53], reducing the proportion of free water available as a reactant and lowering water activity ($a_w < 1$). In Fig. 4A, this appears as a systematic suppression of the model prediction (Γ^{-1}) relative to the variant that omits the water-activity term (Γ^{-1^*}). Calculations (Fig. 4B) indicate that this reduction in a_w is negligible at low ionic strengths but becomes appreciable above 1 mol kg^{-1}, causing a 7% decrease in the overall activity ratio at 2.0 mol kg^{-1}. The equilibrium response therefore reflects two competing effects: electrostatic stabilisation of the ionic products (promoting hydrolysis), and the decline in water activity (moderating this shift). Earlier treatments that focused solely on ionic interactions did not explicitly include this latter contribution, shown here to be significant under concentrated conditions.

3.4. Measured equilibria and non-ideal behaviour in electrolyte media

The influence of the background electrolyte was theoretically examined by replacing $NaClO_4$ with NaCl (Fig. 5) within the framework. In both media, the activity ratio (Γ^{-1}) increased to a maximum ($I_m \approx 0.5$ mol kg^{-1}) and then declined at higher ionic strengths (Fig. 5A). Across the full range, NaCl solutions are expected to exhibit slightly higher Γ^{-1} values, typically within a few percent of those in $NaClO_4$. This consistent difference reflects the smaller ionic radius and stronger hydration of Cl^- relative to the more diffuse ClO_4^- anion. Enhanced hydration and electrostatic stabilisation of Cl^- lower the

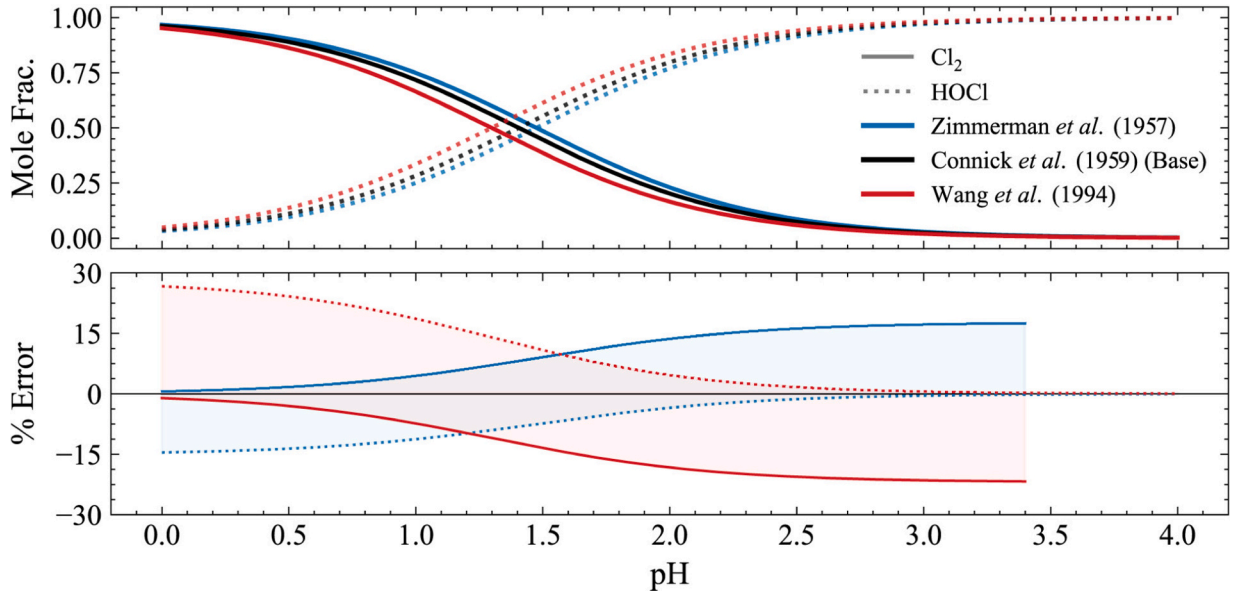

Fig. 3. Calculated chlorine speciation under ideal-solution assumptions ($[Cl^-]_{total} = 0.01$ M, unity activity coefficients) at 298.15 K. The curve illustrates the sensitivity of the equilibrium position to the reported range of thermodynamic equilibrium constants (K^{Θ}). A) Mole fraction of Cl_2 (solid lines) and HOCl (dotted lines) as a function of pH. B) The percentage error in chloride speciation relative to Connick et al. ($K^{\Theta} = 3.944 \times 10^{-4}$)[17]. The equilibrium constants correspond to the range of values reported by Zimmerman et al. ($K^{\Theta} = 3.35 \times 10^{-4}$) [18], and Wang et al. ($K^{\Theta} = 5.05 \times 10^{-4}$) [21].

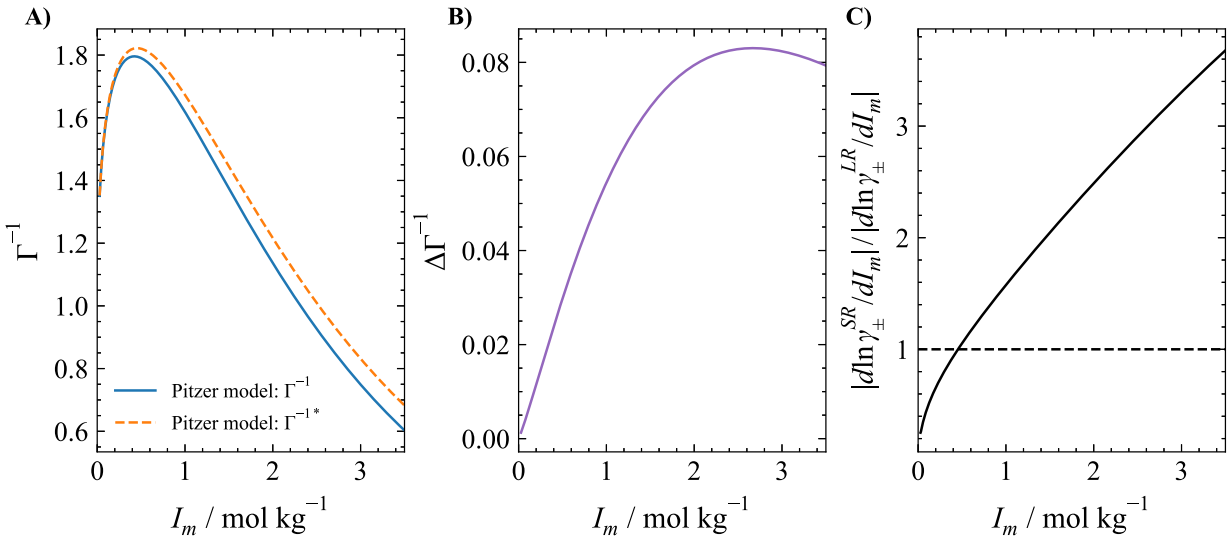

Fig. 4. Decomposition of non-ideal effects on the activity ratio (Γ^{-1}) of chlorine hydrolysis in $NaClO_4$ solutions 298.15 K, with trace H^+ and Cl^- (16 mM). (A) The activity ratio as a function of ionic strength, calculated using the full Pitzer framework, and a variant neglecting water activity (Γ^{-1*}). (B) Difference between the two models $(\Delta\Gamma^{-1})$, showing the specific contribution of water activity to the overall non-ideality. (C) Ratio of the magnitudes of the short-range to long-range contributions to the derivative of the mean activity coefficient of HCl; values exceeding unity indicate dominance of short-range interactions in controlling the ionic strength dependence of $\ln\gamma_{\pm}$.

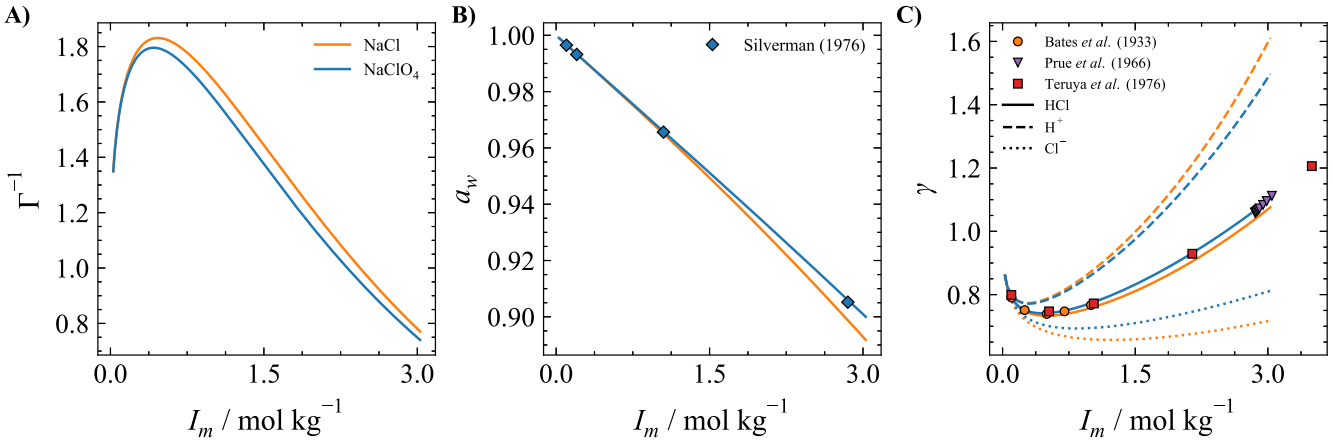

Fig. 5. Calculated theoretical thermodynamic properties for chlorine hydrolysis in $NaClO_4$ (blue line) and NaCl (orange line) background electrolytes at 298.15 K as a function of ionic strength. Theoretical curves are derived from the Pitzer framework assuming trace H^+ and Cl^- (16 mM). (A) The equilibrium activity ratio (Γ^{-1}) for chlorine hydrolysis. (B) Water activity (a_w). Experimental data points represent a reactive chlorine hydrolysis system at 298.15 K, where $NaClO_4$ is used to adjust ionic strength. [20] (C) Mean ionic activity coefficients $(\gamma_{\pm})$ for HCl and model-resolved single-ion components $(\gamma_{H^+}, \gamma_{Cl^-})$ used for thermodynamic decomposition. Experimental data points correspond to literature-reported mean HCl activity coefficients in non-reactive trace HCl-$NaClO_4$ systems at 298.15 K. [46–48]. (For interpretation of the references to colour in this figure legend, the reader is referred to the web version of this article.)

activity-coefficient product $(\gamma_{H^+}\gamma_{Cl^-})$ and thus marginally favour the forward hydrolysis reaction (Eq. 4).

Electrolyte-specific trends are also apparent in the predicted water activity (Fig. 5B). At ionic strengths >1.5 mol kg^{-1}, water activity decreased more rapidly in NaCl than in $NaClO_4$, consistent with the stronger hydration of Cl^- and its greater ability to incorporate water molecules into structured solvation shells. The corresponding ionic activity coefficients (Fig. 5C) indicate that γ_{H^+} increases more rapidly in NaCl, reflecting enhanced short-range repulsion within the more compact hydration environment of Na^+ and Cl^-. In contrast, γ_{Cl^-} rise more sharply in $NaClO_4$, where weaker association with the larger, less hydrated ClO_4^- anion reduces electrostatic screening.

These results suggests that subtle but systematic electrolyte-specific differences in hydration and ion-ion interactions influence the equilibrium position. Within the studied computational concentration range, the Pitzer framework predicts systematic electrolyte-dependent trends.

To establish an experimental basis for evaluating the theoretical framework, chlorine hydrolysis equilibria were measured at 298.15 ± 0.1 K. Two electrolyte systems were examined: $NaClO_4$ over the range of $0.028 \leq I_m \leq 2.1$ mol kg^{-1}. and NaCl over the range of $0.076 \leq I_m \leq 0.83$ mol kg^{-1}. The full experimental methods are detailed in the Supporting Information.

A unified analytical methodology was employed for both systems. Absorbance spectra (A_λ) were analysed using the Beer-Lambert relation. As no optically active complexes are formed between the chlorine species under the conditions studied, the measured absorbance at each wavelength can be treated as the linear sum of the individual species contributions (Eq. 11).

Equilibrium concentrations, including Cl_3^-, were reconstructed from the initial stoichiometry and the full chlorine mass mass balance re-

lations (Eqs. 12–15), with the trichloride formation equilibrium closed using a fixed literature value of $K_{Cl_3^-} = 0.18$ [42]. Concentrations were obtained by weighted, single-parameter least-squares regression of the Cl_2 UV–Vis absorbance data. In the absence of an independent orthogonal analytical constraint (e.g., external chloride or dissolved chlorine quantification), the Cl_2/Cl_3^- equilibrium provides the minimum thermodynamic closure required for a unique and internally consistent speciation reconstruction. Alternative external closures are possible in principle but would require additional independent observables and were therefore outside the scope of the present UV–Vis framework.

A necessary simplification involved omitting the Cl_3^- ion (and its interactions) from the theoretical Pitzer model, the required ion-interaction parameters are unavailable in the literature, highlighting a limitation of the Pitzer model. The impact of this omission is system dependent. In the $NaClO_4$ system, the low chloride concentration resulted in a negligible calculated Cl_3^- concentration (< 0.025 mM). In the NaCl system, the concentration was greater (up to 1.5 mM); however, as this contributed minimally to the total ionic strength (< 0.2%), its omission from the Pitzer framework is considered a justifiable source of model uncertainty.

$$A_\lambda = \sum_j \left(\varepsilon_{j,\lambda} c_j l\right), \tag{11}$$

$$[HOCl]_\infty = [HOCl]_0 - [Cl_2]_\infty \tag{12}$$

$$[Cl^-]_\infty = \frac{[Cl^-]_0 - [Cl_2]_\infty}{\left(1 + K_{Cl_3^-}\,[Cl_2]_\infty\right)} \tag{13}$$

$$[H^+]_\infty = [H^+]_0 - [Cl_2]_\infty \tag{14}$$

$$\left[Cl_3^-\right]_\infty = K_{Cl_3^-}[Cl^-]_\infty[Cl_2]_\infty \tag{15}$$

A consideration in the analysis was the known ionic-strength dependence of the HOCl molar extinction coefficient. For $NaClO_4$ solutions, absorbance was corrected using the parameters of Silverman (1976) [20] (Eq. 16, listed in Table S8). This correction enabled a consistent full-spectrum fit across all ionic strengths.

$$\ln(\varepsilon_\lambda) = \ln\left(\varepsilon_\lambda^0\right) - \omega[NaClO_4] \tag{16}$$

Time-course measurements confirmed that the system achieves chemical and thermal equilibrium within 20 min. Accordingly, all subsequent UV–Vis spectra were recorded after this duration (Fig. 6).

The determination of the equilibrium constant was performed in $NaClO_4$ solutions over the full ionic-strength range ($0.028 \le I_m \le 2.1$ mol kg^{-1}) at 298.15 ± 0.1 K. The concentration-based equilibrium quotients, K^c, were calculated using the species concentrations derived from Eqs. 12–14. These quotients were then corrected for non-ideal solution behaviour using the activity ratios (Γ^{-1})

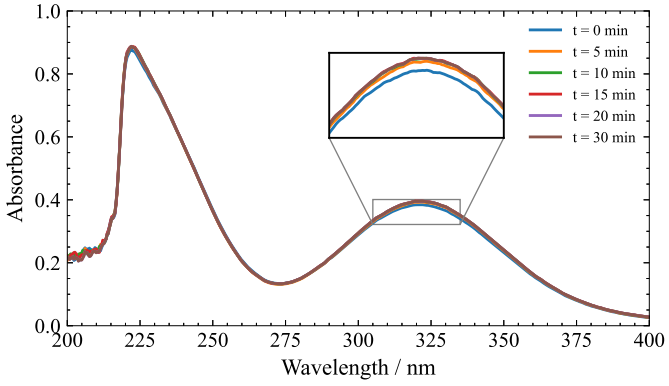

Fig. 6. UV–Vis spectra of chlorine hydrolysis at 298.15 ± 0.1 K and 0.1 mol kg^{-1} ionic strength $NaClO_4$, recorded at successive time intervals.

Table 2
Ionic strength dependence of chlorine hydrolysis equilibrium constant in $NaClO_4$ media at 298.15 ± 0.1 K.

I_m (mol kg^{-1})	$K^c \times 10^4$	Γ^{-1}	$K^\Theta \times 10^4$
2.133	4.24	1.08	3.93
1.713	5.24	1.33	3.94
1.260	6.02	1.53	3.93
1.052	6.39	1.62	3.94
0.837	6.68	1.69	3.95
0.627	6.87	1.74	3.95
0.507	7.14	1.81	3.94
0.313	7.07	1.79	3.95
0.218	7.06	1.79	3.94
0.122	6.63	1.68	3.95
0.028	5.39	1.37	3.93

Note: K^c values represent the mean of three independent experimental replicates. The activity ratio Γ^{-1} was calculated using the Pitzer model [31–34] was used to determine the thermodynamic equilibrium constant via $K^\Theta = K^c/\Gamma^{-1}$. Uncertainties reported correspond to the 95% confidence interval. For all experiments, initial concentrations were $[HCl]_0 = 33.33$ mM and $[NaOCl]_0 = 9.87$ mM. Assuming K^Θ is independent of ionic strength, the pooled mean across all conditions is $K^\Theta = (3.94 \pm 0.01) \times 10^{-4}$ ($n = 11$).

from Eq. 10, with ionic and solvent activity calculated from the Pitzer framework (Eqs. S1-S17). The resulting values are reported in Table 2.

The relationship between the experimental and Pitzer-derived Γ^{-1} are shown in Fig. 7. The results reveal the non-monotonic behaviour calculated by the Pitzer framework: the activity ratio increases to a maximum value of 1.81 at approximately 0.5 mol kg^{-1}, before decreasing at higher concentrations. This pattern reflects the predicted balance between electrostatic stabilisation of the ionic products at low ionic strengths ($I_m \le 0.5$ mol kg^{-1}), and the opposing effects of short-range repulsion and reduced water activity at higher concentrations ($I_m \ge 0.5$ mol kg^{-1}).

The correspondence between the experimental data and the calculated values, with a mean deviation of 1.5%, indicates that the Pitzer framework provides an internally consistent description of the thermodynamic effects governing chlorine hydrolysis under the examined ionic strength range ($0.028 \le I_m \le 2.1$ mol kg^{-1}), at 298.15 K.

The chlorine hydrolysis equilibrium was subsequently examined in NaCl solutions ($0.076 \le I_m \le 0.828$ mol kg^{-1}) to assess the ion-specific effects anticipated by the Pitzer framework (Fig. 8). As established in the methodology, the Cl_3^- concentration was larger in the present system; this was accounted for in the experimentally determined K^c values. A full, parallel assessment of the Pitzer framework's self-consistency for the non-reactive $NaCl - HCl - H_2O$ proxy system was also performed and is detailed in the Supporting Information (Fig. S3), confirming the model's applicability for this electrolyte as well. The results are summarised in Table 3.

As shown in Fig. 8, the measured activity ratios in NaCl were consistently, though only slightly, higher than those in $NaClO_4$ at equivalent ionic strengths. This difference mirrors the trend calculated by the Pitzer framework and is attributed to the stronger electrostatic stabilisation of the H^+ and Cl^- product ions by the smaller, more highly hydrated Cl^- background anion, compared to the large diffuse ClO_4^-. Enhanced hydration of Cl^- lowers the mean activity coefficient product ($\gamma_{H^+}\gamma_{Cl^-}$), and thereby marginally favours the forward hydrolysis reaction (Eq. 4).

$K^\Theta = 3.94 \times 10^{-4}$ at 298.15 K was determined previously in this work and used as the thermodynamic reference state for calculation of the activity ratio $\Gamma^{-1} = K^c/K^\Theta$. For each condition, reported K^c values represent the mean of three independent experiments. The corresponding uncertainties in Γ^{-1} reflect propagation of the experimental uncertainty in the mean K^c, evaluated at the 95% confidence level.

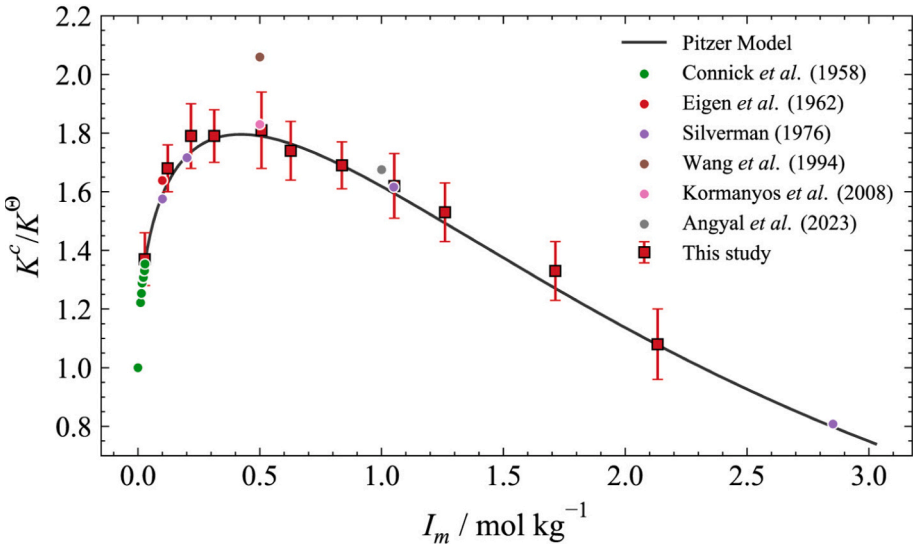

Fig. 7. Experimental results and corresponding calculations from the Pitzer framework for chlorine hydrolysis within a $NaClO_4$ media at 298.15 ± 0.1 K. Initial concentrations were $[HCl]_0 = 33.33$ mM and $[NaOCl]_0 = 9.87$ mM. Literature data: Eigen et al. [19] and Kormanyos et al. [54] (both adjusted for the graphical error in Eigen et al.); Wang et al. $(K^\Theta = 5.05 \times 10^{-4})$. [21] All other literature values correspond to $K^\Theta = 3.944 \times 10^{-4}$. Data taken from sources [17,19–21,54,55].

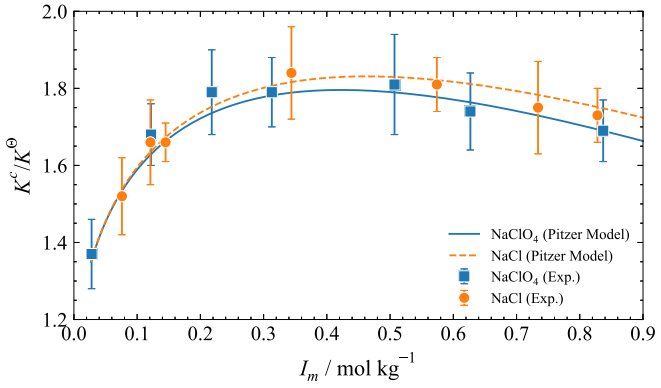

Fig. 8. Comparison of calculated and experimental activity ratios (Γ^{-1}) for chlorine hydrolysis at 298.15 ± 0.1 K. The dependence of Γ^{-1} on ionic strength is shown for sodium perchlorate and sodium chloride electrolytes. Initial concentrations were $[HCl]_0 = 33.33$ mM, with $[NaOCl]_0 = 9.86$ mM for the $NaClO_4$ system and 10.5 mM for the NaCl system.

Table 3
Experimentally determined activity ratios of chlorine hydrolysis in NaCl solutions at 298.15 ± 0.1 (K).

I_m (mol kg^{-1})	$K^c \times 10^4$	K^c/K^Θ
0.076	6.01	1.52 ± 0.10
0.120	6.53	1.66 ± 0.11
0.145	6.55	1.66 ± 0.05
0.344	7.26	1.84 ± 0.12
0.574	7.12	1.81 ± 0.07
0.734	6.92	1.75 ± 0.12
0.828	6.82	1.75 ± 0.07

Initial concentrations were $[NaOCl]_0 = 10.5$ mM, $[HCl]_0 = 33.33$ mM.

The consistent difference between the two electrolytes supports the interpretation that specific-ion effects, rather than general ionic-strength effects, influence the equilibrium. The measured trends are reproduced by the Pitzer calculations within experimental uncertainty, reinforcing that the framework captures the dominant thermodynamic factors controlling chlorine hydrolysis under the examined ionic strength range ($0.076 \leq I_m \leq 0.828$ mol kg^{-1}) at 298.15 K. The Pitzer framework reproduces these electrolyte-specific deviations using standard ion-interaction parameters, confirming its utility for estimating behaviour in mixed industrial anolytes where empirical correlations often falter.

The application of a Pitzer-consistent framework to the chlorine hydrolysis equilibrium provides a structured method for accounting for the ionic environments. By determining the thermodynamic equilibrium constant (K^Θ) and evaluating the relevant specific-ion parameters, this study establishes an experimental basis for modelling speciation beyond the limits of ideal-solution approximations.

However, the model in its current form relies on necessary simplifications. The interaction parameters for neutral species (Cl_2 HOCl) and the trichloride ion (Cl_3^-) are not currently available in the literature. Therefore, they were omitted from the present analysis. This restricts the immediate applicability of the model to conditions where the accumulation of trichloride and the salting-out of neutral species are minimal. The assumption of unit activity coefficients for these species appears sufficient to describe the experimental data within the ionic strengths examined here. However, it is likely insufficient for highly concentrated industrial brines where specific interactions involving these species becomes significant.

The relevance of the present results to chlor-alkali systems lies in the thermodynamic structure of the equilibrium response rather than in direct numerical transferability to electrolyser operating temperatures. By establishing a consistent reference description at 298.15 K, the competing contributions of electrostatic interactions and solvent activity can be resolved independently of temperature-dependent effects. Extension of the framework to elevated temperatures would require re-parameterisation of activity coefficients and water activity using dedicated high-temperature measurements. Such extension is beyond the scope of the present work but follows directly from the methodology established here.

The ability of the framework to describe chlorine hydrolysis equilibria in both $NaClO_4$ and NaCl media highlights the adaptability of the approach. The agreement observed across these distinct ionic environments suggests that the method captures the dominant specific-ion effects regardless of the background anion. This indicates that the framework is applicable to other background electrolytes commonly encountered in process engineering. It may also offer a template for analysing other coupled equilibrium reactions where activity coefficient

corrections are crucial. However, further studies will be required to determine the specific interaction parameters for these broader systems and to verify the method's applicability to additional multi-component mixtures.

4. Conclusion

The chlorine hydrolysis equilibrium, a key reaction in industrial chlor-alkali processes, was examined under concentrated electrolyte conditions using a combined experimental and theoretical approach. All equilibrium measurements occur at finite ionic strength, and interpretation therefore depends on how non-ideal solution behaviour is treated. Equilibrium measurements obtained at 298.15 ± 0.1 K in sodium perchlorate and sodium chloride media were analysed using explicit activity and solvent corrections. A thermodynamic equilibrium constant of $K^{\Theta} = (3.94 \pm 0.01) \times 10^{-4}$ was obtained under explicit treatment of ionic and solvent non-ideality. As this value is derived under the necessary assumption of unit activity coefficients for neutral species, it is rigorously defined as an upper bound within the concentration range investigated.

The resulting thermodynamic equilibrium constant is consistent with early determinations [17] obtained under dilute or weakly non-ideal conditions. This agreement indicates that, when finite ionic strength effects are treated explicitly, the underlying thermodynamic reference state is recovered reproducibly. In contrast, the divergence among values commonly used in more recent applied studies reflects differences in how non-ideal effects are incorporated, rather than changes in the intrinsic equilibrium itself. Apparent discrepancies therefore arise when equilibrium constants evaluated at finite ionic strength are transferred or compared without consistent treatment of activity and solvent contributions.

Analysis of the equilibrium behaviour shows that deviations from ideality are governed primarily by the response of the charged products (H^+ and Cl^-) to the ionic environment, together with changes in water activity. These contributions dominate the apparent equilibrium position across the studied ionic strength range and give rise to a non-monotonic dependence on ionic strength. Within this range, the approximation of unity activity coefficients for neutral species is supported, while explicit treatment of ionic and solvent effects is required to maintain thermodynamic consistency.

Equilibrium measurement conducted in sodium perchlorate and sodium chloride electrolytes further show that the equilibrium position depends not only on ionic strength but also electrolyte composition. Direct comparison between the two media reveals small but reproducible shifts attributable to differences in anion hydration and specific ion interactions, indicating that ionic strength alone does not fully capture equilibrium behaviour in concentrated electrolytes.

By distinguishing intrinsic equilibrium behaviour from electrolyte-dependent non-ideal effects, a thermodynamically well-defined reference description for chlorine hydrolysis at 298.15 K is obtained. This separation provides a clear basis for interpreting chlorine speciation in concentrated aqueous systems and for assessing how background electrolyte composition and ionic strength influence equilibrium behaviour in process-relevant speciation modelling. In this context, the framework enables screening of ionic strength regimes and background electrolytes that provide desirable equilibrium conditions, which is relevant for process analysis and optimisation in chlor-alkali systems.

Although the present work is restricted to chlorine hydrolysis, the underlying thermodynamic approach is general in form. Its application to other reactive aqueous systems may be possible where suitable interaction parameters are available, although further experiment and thermodynamic investigation would be required to establish its validity beyond the system examined here.

CRediT authorship contribution statement

Lewis A.D. Waller: Writing – review & editing, Writing – original draft, Visualization, Validation, Software, Methodology, Investigation, Formal analysis, Data curation. **Andrea E. Russell:** Writing – review & editing, Supervision, Resources. **Peter P. Wells:** Writing – review & editing, Supervision, Resources. **Richard G. Wills:** Writing – review & editing, Supervision, Resources. **Robert Raja:** Writing – review & editing, Supervision, Resources, Project administration, Funding acquisition, Conceptualization. **Lindsay-Marie Armstrong:** Writing – review & editing, Writing – original draft, Supervision, Resources, Project administration, Funding acquisition, Conceptualization.

Declaration of competing interest

The authors declare that they have no known competing financial interests or personal relationships that could have appeared to influence the work reported in this paper.

Acknowledgements

The authors gratefully acknowledge P. Birkin for reviewing the experimental methods for UV–Vis accuracy, M. P. Stockham for valuable scientific discussions, and N. Garcia-Araez for providing lab space and equipment.

This project was supported with funding from Southampton Marine & Maritime Institute (SMMI) Studentship and EPSRC DTP 2022 (EP/W524621/1).

Appendix A. Supplementary data

Supplementary data to this article can be found online at https://doi.org/10.1016/j.cej.2026.174476.

Data availability

Data will be made available on request.

References

[1] M. Carvela, J. Lobato, and M. A. Rodrigo, "Chloralkali low temperature PEM reversible electrochemical cells," Electrochim. Acta, vol. 387, pp. 138542–138542, 2021/8// 2021, doi:https://doi.org/10.1016/J.ELECTACTA.2021.138542.

[2] F. Klaucke, C. Hoffmann, M. Hofmann, and G. Tsatsaronis, "Impact of the chlorine value chain on the demand response potential of the chloralkali process," Appl. Energy, vol. 276, pp. 115366–115366, 2020/10// 2020, doi:https://doi.org/10.1016/J.APENERGY.2020.115366.

[3] K. Li, Q. Fan, H. Chuai, H. Liu, S. Zhang, X. Ma, Revisiting Chlor-alkali Electrolyzers: from materials to devices, Transactions of Tianjin University 27 (3) (2021) 202–216, https://doi.org/10.1007/s12209-021-00285-9.

[4] H. Ritchie, P. Rosado, and M. Roser, "Breakdown of Carbon Dioxide, Methane and Nitrous Oxide Emissions by Sector," in *our World in Data*, Ed, 2020.

[5] J. Huang *et al.*, "RuO2 nanoparticles decorate belt-like anatase TiO2 for highly efficient chlorine evolution," Electrochim. Acta, vol. 339, pp. 135878–135878, 2020/4// 2020, doi:https://doi.org/10.1016/J.ELECTACTA.2020.135878.

[6] Y. Cheng *et al.*, "Boosting selective chlorine evolution reaction: impact of ag doping in RuO2 electrocatalysts," J. Colloid Interface Sci., vol. 685, pp. 97–106, 2025/5// 2025, doi:https://doi.org/10.1016/J.JCIS.2025.01.097.

[7] R. AgileIntel, "Chlorine Global Market Volume 2030 | Statista," in *Market Volume of Chlorine Worldwide from 2015 to 2022, with a Forecast for 2023 to 2030 (in Million Metric Tons) [Graph]*, Ed, 2023.

[8] R. K. B. Karlsson and A. Cornell, "Selectivity between oxygen and chlorine evolution in the Chlor-alkali and chlorate processes," Chem. Rev., vol. 116, no. 5, pp. 2982–3028, 2016/3// 2016, doi:https://doi.org/10.1021/acs.chemrev.5b00389.

[9] W. Cheng *et al.*, "RuO2/IrO2 nanoparticles decorated TiO2 nanotube arrays for improved activity towards chlorine evolution reaction," Catal. Today, vol. 400-401, pp. 26–34, 2022/9// 2022, doi:https://doi.org/10.1016/J.CATTOD.2022.04.004.

[10] X. Tang, I. Arif, and P. Diao, "Monitoring the chlorine evolution reaction during electrochemical alkaline seawater splitting," J. Electroanal. Chem., vol. 942, pp. 117569–117569, 2023/8// 2023, doi:https://doi.org/10.1016/J.JELECHEM.2023.117569.

[11] W. R. Leow *et al.*, "Chloride-mediated selective electrosynthesis of ethylene and propylene oxides at high current density," Science, vol. 368, no. 6496, pp. 1228–1233, 2020/6// 2020, doi:https://doi.org/10.1126/science.aaz8459.

[12] Y. Li *et al.*, "Redox-mediated electrosynthesis of ethylene oxide from CO2 and water," *Nat. Catal. 2022 5:3,* vol. 5, no. 3, pp. 185–192, 2022/2// 2022, doi:https://doi.org/10.1038/s41929-022-00749-8.

[13] C. Lucky, T. Wang, and M. Schreier, "Electrochemical ethylene oxide synthesis from ethanol," ACS Energy Lett., vol. 7, no. 4, pp. 1316–1321, 2022/4// 2022, doi:https://doi.org/10.1021/acsenergylett.2c00265.

[14] Q. Li, G. h. Liu, L. Qi, H. Wang, and G. Xian, "Chlorine-mediated electrochemical advanced oxidation process for ammonia removal: mechanisms, characteristics and expectation," Sci. Total Environ., vol. 896, pp. 165169–165169, 2023/10// 2023, doi:https://doi.org/10.1016/J.SCITOTENV.2023.165169.

[15] E. Lacasa, E. Tsolaki, Z. Sbokou, M. A. Rodrigo, D. Mantzavinos, and E. Diamadopoulos, "Electrochemical disinfection of simulated ballast water on conductive diamond electrodes," Chem. Eng. J., vol. 223, pp. 516–523, 2013/5// 2013, doi:https://doi.org/10.1016/J.CEJ.2013.03.003.

[16] S. Zhao *et al.*, "Selective electrosynthesis of chlorine disinfectants from seawater," *Nat. Sustainability 2024 7:2,* vol. 7, no. 2, pp. 148–157, 2024/2// 2024, doi:https://doi.org/10.1038/s41893-023-01265-8.

[17] R. E. Connick, Y.-T. Chía, Yol, and Y.-T. Chía, "The hydrolysis of chlorine and its variation with temperature," J. Am. Chem. Soc., vol. 81, no. 6, pp. 1280–1284, 1959/3// 1959, doi:https://doi.org/10.1021/ja01515a004.

[18] G. Zimmerman and F. C. Strong, "Equilibria and spectra of aqueous chlorine solutions," J. Am. Chem. Soc., vol. 79, no. 9, pp. 2063–2066, 1957/5// 1957, doi:https://doi.org/10.1021/JA01566A011.

[19] M. Eigen and K. Kustin, "The kinetics of halogen hydrolysis," J. Am. Chem. Soc., vol. 84, no. 8, pp. 1355–1361, 1962/4// 1962. [Online]. Available: https://pubs.acs.org/sharingguidelines.

[20] R. A. Silverman, "Variation of Chlorine - Hypochlorous Acid Equilibrium and Spectra with Ionic Strength; Kinetics and Mechanism of the Uranium(Iv)-Hypochlorous Acid Reaction," in *ProQuest Dissertations and Theses*, Ed. Iowa City: The University of Iowa, 1976, pp. 65–92.

[21] T. X. Wang and D. W. Margerum, "Kinetics of reversible chlorine hydrolysis: temperature dependence and general-acid/base-assisted mechanisms," Inorg. Chem., vol. 33, no. 6, pp. 1050–1055, 1994/3// 1994, doi:https://doi.org/10.1021/IC00084A014.

[22] H. Ito, A. Manabe, Chapter 8 - Chlor–alkali electrolysis, in: T. Smolinka, J. Garche (Eds.), Electrochemical Power Sources: Fundamentals, Systems, and Applications, Elsevier, 2022, pp. 281–304.

[23] I. Requena-Leal, M. Carvela, C. M. Fernández-Marchante, J. Lobato, and M. A. Rodrigo, "On the use of chlor-alkali technology to power environmental electrochemical treatment technologies," *Curr. Opin. Electrochem.,* vol. 45, p. 101461, 2024/06/01/ 2024, doi:https://doi.org/10.1016/j.coelec.2024.101461.

[24] N. N. Liang, W. Choi, D. Suk Han, and H. Park, "Electrocatalytic conversion of ethylene to ethylene oxide mediated by halide oxidation: chloride vs. bromide vs. iodide," Chem. Eng. J., vol. 494, pp. 153042–153042, 2024/8// 2024, doi:https://doi.org/10.1016/J.CEJ.2024.153042.

[25] G. L. Squadrito, E. M. Postlethwait, and S. Matalon, "Elucidating mechanisms of chlorine toxicity: reaction kinetics, thermodynamics, and physiological implications," Am. J. Phys. Lung Cell. Mol. Phys., vol. 299, no. 3, pp. L289–L289, 2010/9// 2010, doi:https://doi.org/10.1152/AJPLUNG.00077.2010.

[26] I. Lengyel, J. Li, K. Kustin, I.R. Epstein, Rate constants for reactions between iodine- and chlorine-containing species: a detailed mechanism of the chlorine dioxide/chlorite-iodide reaction, J. Am. Chem. Soc. 118 (15) (1996) 3708–3719, https://doi.org/10.1021/JA953938E.

[27] E. P. Rivero, F. A. Rodríguez, M. R. Cruz-Díaz, and I. González, "Reactive diffusion migration layer and mass transfer wall function to model active chlorine generation in a filter press type electrochemical reactor for organic pollutant degradation," Chem. Eng. Res. Des., vol. 138, pp. 533–545, 2018/10// 2018, doi:https://doi.org/10.1016/J.CHERD.2018.07.010.

[28] J. G. Vos and M. T. M. Koper, "Measurement of competition between oxygen evolution and chlorine evolution using rotating ring-disk electrode voltammetry," J. Electroanal. Chem., vol. 819, pp. 260–268, 2018/6// 2018, doi:https://doi.org/10.1016/J.JELECHEM.2017.10.058.

[29] Y. Zhang *et al.*, "Removal of micropollutants by an electrochemically driven UV/chlorine process for decentralized water treatment," Water Res., vol. 183, pp. 116115–116115, 2020/9// 2020, doi:https://doi.org/10.1016/J.WATRES.2020.116115.

[30] C.Y. Cheng, G.H. Kelsall, Models of hypochlorite production in electrochemical reactors with plate and porous anodes, J. Appl. Electrochem. 37 (11) (2007) 1203–1217, https://doi.org/10.1007/s10800-007-9364-7.

[31] S.L. Clegg, K.S. Pitzer, Thermodynamics of multicomponent, miscible, ionic solutions: generalized equations for symmetrical electrolytes, J. Phys. Chem. 96 (8) (1992) 3513–3520.

[32] K.S. Pitzer, Activity Coefficients in Electrolyte Solutions, Second edition, CRC Press, Boca Raton, 1991.

[33] K. S. Pitzer and G. Mayorga, "Thermodynamics of electrolytes. II. Activity and osmotic coefficients for strong electrolytes with one or both ions univalent," J. Phys. Chem., vol. 77, no. 19, pp. 2300–2308, 1973/9// 1973, doi:https://doi.org/10.1021/j100638a009.

[34] K.S. Pitzer, J.M. Simonson, Thermodynamics of multicomponent, miscible, ionic systems: theory and equations, J. Phys. Chem. 90 (13) (1986) 3005–3009, https://doi.org/10.1021/J100404A042.

[35] A. Kumar, "Reassessment of the binary, ternary, and quaternary interactions in mixed electrolytes from thermodynamic quantities: the systems with uncommon ions containing hydrophobic character," J. Phys. Chem. B, vol. 109, no. 23, pp. 11743–11752, 2005/06/01 2005, doi:https://doi.org/10.1021/jp050012c.

[36] P. Millet, *Chlor-Alkali Technology: Fundamentals, Processes and Materials for Diaphragms and Membranes* (Handbook of Membrane Reactors), Woodhead Publishing, 2013, pp. 384–415.

[37] T.F. O'Brien, T.V. Bommaraju, F. Hine, Chemistry and electrochemistry of the Chlor-alkali process, in: T.F. O'Brien, T.V. Bommaraju, F. Hine (Eds.), Handbook of Chlor-Alkali Technology: Volume I: Fundamentals, Volume II: Brine Treatment and Cell Operation, Volume III: Facility Design and Product Handling, Volume IV: Plant Commissioning and Support Systems, Volume V: Corrosion, Environmental Issues, and Future Development, Springer US, Boston, MA, 2005, pp. 75–386.

[38] M. Carvela, J. Lobato, and M. A. Rodrigo, "Chloralkali low temperature PEM reversible electrochemical cells," Electrochim. Acta, vol. 387, p. 138542, 2021/08/10/ 2021, doi:https://doi.org/https://doi.org/10.1016/j.electacta.2021.138542.

[39] P. M. May and D. Rowland, "Thermodynamic modeling of aqueous electrolyte systems: current status," J. Chem. Eng. Data, vol. 62, no. 9, pp. 2481–2495, 2017/09/14 2017, doi:https://doi.org/10.1021/acs.jced.6b01055.

[40] D. Rowland, E. Königsberger, G. Hefter, and P. M. May, "Aqueous electrolyte solution modelling: some limitations of the Pitzer equations," Appl. Geochem., vol. 55, pp. 170–183, 2015/4// 2015, doi:https://doi.org/10.1016/J.APGEOCHEM.2014.09.021.

[41] D. Rowland and P. M. May, "An investigation of harned's rule for predicting the activity coefficients of strong aqueous electrolyte solution mixtures at 25°C," J. Chem. Eng. Data, vol. 62, no. 1, pp. 310–327, 2017/1// 2017, doi:https://doi.org/10.1021/ACS.JCED.6B00651/ASSET/IMAGES/LARGE/JE-2016-00651C_0007.JPEG.

[42] T. X. Wang, M. D. Kelley, J. N. Cooper, R. C. Beckwith, and D. W. Margerum, "Equilibrium, kinetic, and UV-spectral characteristics of aqueous bromine chloride, bromine, and chlorine species," Inorg. Chem., vol. 33, no. 25, pp. 5872–5878, 1994/12// 1994, doi:https://doi.org/10.1021/IC00103A040.

[43] D. G. Leaist, "Absorption of chlorine into water," J. Solut. Chem., vol. 15, no. 10, pp. 827–838, 1986/10/01 1986, doi:https://doi.org/10.1007/BF00646090.

[44] E. M. Aieta and P. V. Roberts, "Henry constant of molecular chlorine in aqueous solution," J. Chem. Eng. Data, vol. 31, no. 1, pp. 51–53, 1986/01/01 1986, doi:https://doi.org/10.1021/je00043a017.

[45] D. Kirk Nordstrom, "Models, validation, and applied geochemistry: issues in science, communication, and philosophy," Appl. Geochem., vol. 27, no. 10, pp. 1899–1919, 2012/10/01/ 2012, doi:https://doi.org/https://doi.org/10.1016/j.apgeochem.2012.07.007.

[46] J. E. Prue and A. J. Read, "Constant ionic media; activity coefficients for hydrogen chloride in aqueous sodium perchlorate," Journal of the Chemical Society A: Inorganic, Physical, Theoretical, no. 0, pp. 1812–1814, 1966/1// 1966, doi:https://doi.org/10.1039/J19660001812.

[47] S. J. Bates and J. W. Urmston, "The activity coefficients of hydrochloric acid in aqueous solutions containing either sodium or potassium perchlorate," J. Am. Chem. Soc., vol. 55, no. 10, pp. 4068–4073, 1933/10// 1933, doi:https://doi.org/10.1021/JA01337A023.

[48] K. Teruya, K. Shiraogawa, and I. Nakamori, "Activity coefficients of hydrochloric acid in hydrogen chloride-metal perchlorate-water systems," Bull. Chem. Soc. Jpn., vol. 49, no. 4, pp. 894–898, 1976/4// 1976, doi:https://doi.org/10.1246/bcsj.49.894.

[49] C.W. Davies, 397. The extent of dissociation of salts in water. Part VIII. An equation for the mean ionic activity coefficient of an electrolyte in water, and a revision of the dissociation constants of some sulphates, Journal of the Chemical Society (Resumed) (1938) 2093–2098.

[50] A. J. Bard, R. Parsons, and J. Jordan, Standard Potentials in Aqueous Solution. Taylor & Francis, 1985.

[51] W. Lai *et al.*, "Differentiating reactive chlorine species for micropollutant abatement in chloride containing water by electrochemical oxidation process," Water Res., vol. 271, pp. 122984–122984, 2025/3// 2025, doi:https://doi.org/10.1016/J.WATRES.2024.122984.

[52] H. W. Nesbitt, "The stokes and Robinson hydration theory: a modification with application to concentrated electrolyte solutions," J. Solut. Chem., vol. 11, no. 6, pp. 415–422, 1982/6// 1982, doi:https://doi.org/10.1007/BF00649040.

[53] K. Gilbert, P. C. Bennett, W. Wolfe, T. Zhang, and K. D. Romanak, "CO2 solubility in aqueous solutions containing Na+, Ca2+, cl−, SO42− and HCO3-: the effects of electrostricted water and ion hydration thermodynamics," Appl. Geochem., vol. 67, pp. 59–67, 2016/4// 2016, doi:https://doi.org/10.1016/J.APGEOCHEM.2016.02.002.

[54] B. Kormányos, I. Nagypál, G. Peintler, and A. K. Horváth, "Effect of chloride ion on the kinetics and mechanism of the reaction between chlorite ion and Hypochlorous acid," Inorg. Chem., vol. 47, no. 17, pp. 7914–7920, 2008/9// 2008, doi:https://doi.org/10.1021/ic8006684.

[55] D. Angyal, I. Fábián, and M. Szabó, "Kinetic role of reactive intermediates in controlling the formation of chlorine dioxide in the hypochlorous acid–chlorite ion reaction," Inorg. Chem., vol. 62, no. 14, pp. 5426–5434, 2023/4// 2023, doi:https://doi.org/10.1021/acs.inorgchem.2c04329.